Editors choice paper

Quantitative relationship between the nature of surface species and the catalytic activity of tungsten oxides supported on crystallized titania

Thomas Onfroy, Vanessa Lebarbier, Guillaume Clet, Marwan Houalla*

Laboratoire Catalyse et Spectrochimie, ENSICAEN, Université de Caen, CNRS, 6 Boulevard du Maréchal Juin, 14050 Caen, France

ARTICLE INFO

ABSTRACT

A series of WO_x/TiO_2 catalysts containing between 0.6 and 3.4 W at./nm^2 was prepared by pore volume impregnation using ammonium metatungstate solution on crystallized TiO_2. Characterization of the solids by X-ray diffraction, Raman and infrared spectroscopy indicated that the W phase was present essentially as a surface W species. The results also suggested an increased degree of condensation of the W phase with increasing W surface density. The most condensed W species was characterized by a $\nu(W=O)$ vibration at 1017 cm^{-1}.

The IR or Raman bands attributed to specific surface species of the solids were correlated with the abundance of relatively strong Brønsted acid sites and isopropanol dehydration activity. A direct correlation was observed between propene formation rate and the area of the band at 1017 cm^{-1}, attributed to the most condensed W species. Furthermore, the abundance of this species appeared to be directly related to that of Brønsted acid sites capable of retaining 2,6-dimethyl pyridine (lutidine) following desorption at 573 K. The behavior of the WO_x/TiO_2 system was compared with that reported for the corresponding WO_x/ZrO_2 solids. Higher intrinsic activity (activity per W atom) was observed for WO_x/TiO_2 system.

© 2009 Elsevier B.V. All rights reserved.

1. Introduction

Supported tungsten oxides catalyze a large number of industrially important reactions including hydrodesulfurization [1,2], metathesis [3,4] and isomerization [5–8]. Specifically, WO_x/TiO_2 system has found application as catalysts for alkene isomerization [9,10]. The system has received an added interest as catalysts (or catalysts precursors) for the reaction of selective catalytic reduction of NO_x by ammonia (SCR process) [11–14]. It has also been shown that WO_x/TiO_2 catalysts are active for photocatalytic decomposition of some organic pollutants [15,16]. Thus a significant number of studies have examined the structure, acidity or catalytic performance of WO_x/TiO_2 solids [17–38]. The formation of a surface W phase for W loadings below the nominal value for monolayer coverage (4.5 W at./nm^2) has been established [29,33,39]. The increased formation of polymeric W species with increasing W surface density has been noted [25,27,32]. The development of Brønsted acidity on W deposition has also been observed [10,11,34,35]. However, few studies have attempted a *quantitative relationship* between surface structure, acidity and catalytic performance [36,37].

The present study is a part of a systematic investigation of the acidity/surface structure/catalytic performance relationships for zirconia- and titania-supported oxides of groups 5 and 6 transition metals. The purpose of the paper is to undertake a detailed analysis of the surface species of WO_x/TiO_2 catalysts as a function of the W surface density. The results, thus obtained, will be correlated with the development of Brønsted acidity and the catalytic performance for an acid-catalyzed reaction which were detailed in a previous work [35]. The overall behavior of the WO_x/TiO_2 system will be compared with that reported for the corresponding zirconia-supported catalysts.

2. Experimental

2.1. Synthesis of WO_x/TiO_2 catalysts

The titania support (Degussa; P-25) was first calcined at 823 K for 24 h. WO_x/TiO_2 samples were prepared by incipient wetness impregnation of TiO_2 with an aqueous solution of ammonium metatungstate $((NH_4)_6H_2W_{12}O_{40})$. The solids were then dried at 393 K for 16 h and calcined in air at 773 K for 16 h. Supported tungsten will be designated as Wx T where x represents the W surface density in atom/nm^2.

2.2. BET surface area

Nitrogen adsorption was measured at 77 K with an automatic adsorptiometer (Micromeritics ASAP 2000). The samples were pretreated at 573 K for 2 h under vacuum. The surface areas were determined from adsorption values for five relative pressures (P/P_0)

---

* Corresponding author. Tel.: +33 2 31 56 73 51; fax: +33 2 31 45 28 22.
E-mail address: marwan.houalla@ensicaen.fr (M. Houalla).

ranging from 0.05 to 0.2 using the BET method. The pore volumes were determined from the total amount of N_2 adsorbed between $P/P_0 = 0.05$ and $P/P_0 = 0.98$.

2.3. X-ray diffraction

X-ray powder diffraction spectra were recorded using a Philips X'pert diffractometer with copper anode ($K\alpha_1 = 0.15405$ nm) and a scanning rate of $0.025°$ s^{-1}. Experimental details can be found in a previous paper [35].

2.4. Raman spectroscopy

Raman characterization was performed on samples exposed to ambient conditions or following dehydration. The samples were dehydrated in a N_2–O_2 (75%–25%) flow at 723 K for 2 h. They were, then, transferred to the Raman cell, in a glove box, under controlled atmosphere (N_2). Raman spectra were recorded with a dispersive Raman (Kaiser) equipped with a diode laser source ($\lambda = 532$ nm) and a CCD detector. The spectra were acquired after 20 10-s scans.

The intensities of the ν(W=O) bands at 1019, 1015 and 1006 cm^{-1} were determined using a linear background for the overall spectral region. The relative contributions of various ν(W=O) bands were estimated from their area after normalization of the spectra with respect to the anatase band at 636 cm^{-1}. Bands areas were obtained by curve-fitting using a Gaussian profile. For curve-fittings, the positions were kept nearly constant (± 1 cm^{-1}) and the FWHM was equal to 10.5 ± 0.5 cm^{-1}.

2.5. Infrared spectroscopy

The IR spectra were recorded with a Nicolet Magna 550 FT-IR spectrometer (resolution: 4 cm^{-1}, 128 scans). All the spectra presented here were normalized for 100 mg of the solid. Samples were pressed into pellets (ca. 20 mg for a 2 cm^2 pellet) and activated at 723 K. The samples were first heated under vacuum at 623 K for 30 min. This was followed by a treatment in O_2 ($P_{equilibrium} = 13.3$ kPa) for 1 h, and evacuation for 30 min at 623 K before cooling down to room temperature (R.T.).

The intensities of the ν(W=O) bands at 1017, 1012 and 1004 cm^{-1} were determined using a linear background for the overall spectral region. The relative contributions of various ν(W=O) bands were estimated from their area after normalization of the spectra to 100 mg of sample. Bands area were obtained by curve-fitting using the parameters used for the curve-fitting of Raman spectra. The attribution of the bands used for curve-fittings was based on the following criteria: (i) the evolution of the spectra with loadings, (ii) the 2nd derivatives, (iii) the comparison between IR and Raman results and (iv) the comparison with the results obtained in a previous work on tungstated zirconia [40].

2,6-Dimethylpyridine (lutidine) was introduced at R.T. ($P_{equilibrium} = 133$ Pa), after activation. The spectra were then recorded following desorption from 323 to 573 K. The number of Brønsted acid sites titrated by 2,6-dimethylpyridine was calculated using an integrated molar absorption coefficient value

of $\varepsilon = 6.8$ cm μmol^{-1} for the sum of the ($\nu_{8a} + \nu_{8b}$) vibrations of protonated lutidine (DMPH$^+$) at ca. 1644 and 1628 cm^{-1} [41].

2.6. Catalytic activity

The catalytic conversion of propan-2-ol (isopropanol) was measured in a fixed bed flow reactor. 100 mg of sample were pretreated at 723 K in N_2 for 2 h (ramp 5 K min^{-1}; 60 cm^3 min^{-1}). The reaction was performed at atmospheric pressure with N_2 as carrier gas ($P_{isopropanol} = 1.23$ kPa; WHSV = 17.3 mmol h^{-1} g^{-1}; total flow rate = 60 cm^3 min^{-1}) at 403 and 413 K. Reactants and products were analyzed with an on line G.C. (HP 5890 Series II) equipped with a capillary column (CP WAX 52 CB) and a FID detector.

3. Results

3.1. Synthesis and composition of WO$_x$/TiO$_2$ catalysts

A series of solids with W contents ranging from 0.80 to 4.80 wt.% was prepared by incipient wetness impregnation on titania. The maximum loading was chosen to avoid the eventual presence of bulk WO$_3$. Table 1 reports the characteristics of the catalysts. The surface area and pore volume of the solids were little affected by W deposition. Therefore, W surface densities were calculated on the basis of the surface area of the titania support. The theoretical coverage was calculated assuming that a full monolayer corresponds to 4.9 W at./nm^2 [42,43]. XRD characterization was reported in a previous work [35]. All the solids showed approximately the same crystalline composition, ca. 60% anatase–40% rutile. Bulk WO$_3$ was not observed.

3.2. Raman spectroscopy

Raman spectra for the titania support and WO$_x$/TiO$_2$ solids, showed, in the 200–800 cm^{-1} region, three bands at 636, 515 and 396 cm^{-1} characteristic of anatase and a band at 447 cm^{-1} attributed to rutile [44]. In accord with the XRD results, the crystalline composition of titania was not modified on tungsten deposition. Although bulk WO$_3$ can be easily detected by Raman spectroscopy because of its high scattering cross-section, no peaks characteristic of WO$_3$ (bands at 806 and 713 cm^{-1}) [39] were observed for all catalysts.

Raman spectra of the WO$_x$/TiO$_2$ solids, obtained after activation in air flow at 723 K, show a band between 990 and 1030 cm^{-1}, characteristic of ν(W=O) vibration of monooxo tungstate species (Fig. 1a) [20,25,45]. Fig. 1b shows that the area of the envelope characteristic of ν(W=O) vibration increases steadily with W surface density.

Examination of the spectra of Fig. 1a indicates the presence of two bands at 1015 and 1006 cm^{-1}. In addition to those bands, curve-fitting of the envelope indicates the presence of a band at 1019 cm^{-1}. A typical example of the decomposition is shown in Fig. 2a for the W3.4 T solid. The presence of a high wavenumber band evidenced by curve-fitting is consistent with the results obtained for the WO$_x$/ZrO$_2$ system [40].

Table 1
Characteristics of WO$_x$/TiO$_2$ catalysts.

Sample	TiO$_2$	W0.6 T	W1.1 T	W1.7 T	W2.3 T	W2.8 T	W3.4 T
Surface area (m^2 g^{-1})	46	47	47	47	47	47	46
Pore volume (cm^3 g^{-1})	0.24	0.25	0.24	0.25	0.24	0.23	0.24
Wt.% W	0	0.80	1.60	2.40	3.20	4.00	4.80
Wt.% WO$_3$	0	1.01	2.02	3.03	4.04	5.05	6.06
W atoms/nm^2	0	0.6	1.1	1.7	2.3	2.8	3.4
% of monolayer	0	12	22	35	47	57	69
% of anatase	58	60	58	59	61	63	57
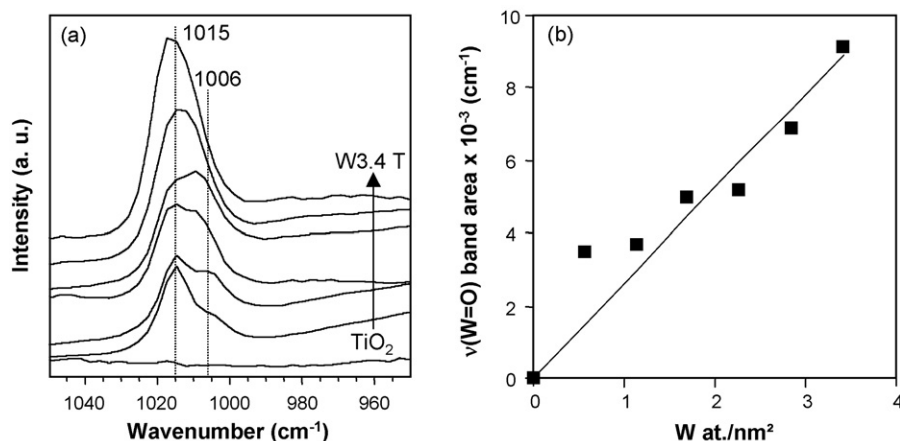
Fig. 1. (a) Raman spectra for titania and WO_x/TiO_2 catalysts pretreated in dry air at 723 K (spectra normalized to the 636 cm^{-1} anatase band). (b) Evolution of the $\nu(W{=}O)$ band area with W surface density.

Fig. 2b represents the evolution of the areas of the bands at 1019, 1015 and 1006 cm^{-1} with W surface density. With increasing W surface density, the intensity of the band at 1006 cm^{-1} first increases, reaches a maximum for 1.7 W at./nm^2 and then decreases for higher surfaces densities whereas that of the band at 1015 cm^{-1} increases steadily with W surface density. Note that the band at 1019 cm^{-1} was only detected for W surface densities $\geq$1.7 W at./nm^2. Its intensity increases steadily with increasing W surface density.

3.3. Infrared spectroscopy

Fig. 3a shows the infrared spectra for the WO_x/TiO_2 solids following evacuation at 623 K. They indicate the presence of a broad envelope in the 990–1040 cm^{-1} region characteristic of $\nu(W{=}O)$ vibration of surface monooxo tungstates species [10,21,34]. In accord with Raman results (Fig. 1a), the area of the band increases linearly with W surface density (Fig. 3b). Despite their low intensity, the overtone bands for the $\nu(W{=}O)$ vibration were observed in the 2000–2040 cm^{-1} region (not shown). Depending on the solid, two bands around 2005–2011 cm^{-1}; 2018–2026 cm^{-1} and a small shoulder at ca. 2034–2036 cm^{-1} were detected. They were consistent with $\nu(WO)$ bands at ca. 1004, 1012 and 1017 cm^{-1}.

A typical example for curve-fitting the envelope in the 990–1040 cm^{-1} region is shown in Fig. 4 for W0.6T and W3.4T catalysts. Also included in the figure, are the 2nd derivatives of the experimental spectra. In addition to the main peak at 1012 cm^{-1},

shoulders at 1002 and 1016 cm^{-1} were evidenced in the 2nd derivatives. Thus three bands at 1004, 1012 and 1017 cm^{-1} were used for curve-fitting the spectra (see Section 2 for more details). A good agreement between experimental and reconstituted spectra is observed.

Fig. 5 represents the variation of the areas of various bands $\nu(W{=}O)$ as a function of W surface density. The area of the low wavenumber band at 1004 cm^{-1} increases up to 1.7 W/nm^2 and appears to level off for higher W densities whereas that of the band at 1012 cm^{-1} shows a steady increase. The band at 1017 cm^{-1} was first detected for the solid W1.7/Ti. Its area progressively increases with W. Note that the evolution of the areas of the various bands is consistent with that observed by Raman spectroscopy (Fig. 2b).

The region characteristic of the OH vibration (3800–3500 cm^{-1}) was also examined. The observed bands were of low intensity which prevented any detailed analysis of the spectra. It was, however, clear that the overall intensity of the OH bands decreases with tungsten loading, evidencing the consumption of the TiO$_2$ hydroxyls on W deposition.

4. Discussion

4.1. Preparation of the catalysts

Textural and structural characterization of WO_x/TiO_2 catalysts by BET, XRD and Raman spectroscopy shows no significant effect of W deposition on the surface area and the composition of the
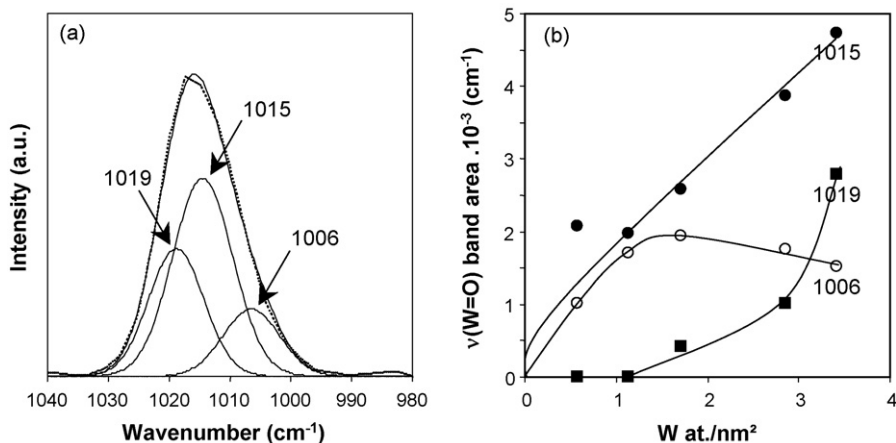
Fig. 2. (a) Curve-fitting of the Raman spectra of the $\nu(W{=}O)$ band for W3.4 T (dashed line: experimental spectrum; full line: curve-fitted spectra); (b) evolution of the area of the $\nu(W{=}O)$ band measured at 1019 (■), 1015 (●) and 1006 (○) cm^{-1} with W surface density of WO_x/TiO_2 solids.
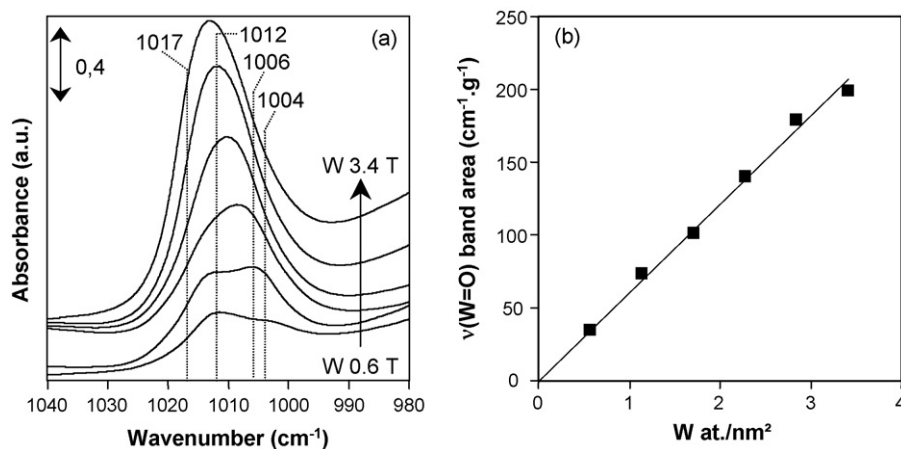
Fig. 3. (a) Infrared spectra for WO_x/TiO_2 catalysts activated in vacuum at 623 K (spectrum of TiO_2 subtracted); (b) Evolution of the $\nu(W{=}O)$ band area (measured between 990 and 1030 cm^{-1} and normalized to 1 g of catalyst) with W surface density.

support (anatase/rutile ratio). XRD and Raman spectroscopy also show no evidence of bulk WO_3 phase, indicating the high dispersion of the supported W phase. This is in agreement with the literature which reports the absence of WO_3 for W surface densities up to 3.5–3.8 W at./nm^2 (70–80% monolayer) [20,39,45].

4.2. Structure of surface W species

The lack of evidence for WO_3 formation and the progressive increase observed for the areas of the Raman (Fig. 1b) and infrared bands (Fig. 3b) characteristic of surface W species, indicate the development of WO_x surface species with increasing W surface density. This is consistent with XPS [18,20,39], ISS [24] and EXAFS [46] measurements.

The study of the envelope characteristic of $\nu(W{=}O)$ vibration attributed to surface monooxo tungstate species indicates the presence of three bands at 1019, 1015 and 1006 cm^{-1} by Raman spectroscopy and at 1017, 1012 and 1004 cm^{-1} by infrared spectroscopy. It is interesting to note that previous in situ Raman study by Wachs et al. [20,25] have reported the presence of one band at 1010 cm^{-1}. However, the spectra reported by the authors for the

sample with low W surface density (ca. 0.5 W at./nm^2) do show the presence of a shoulder at ca.1000 cm^{-1}.

Several infrared bands at ca. 1020, 1017, 1010 and 1002 cm^{-1} were also detected for tungstated titania (i.e. solids obtained by impregnation of titanium hydroxide $Ti(OH)_4$) and calcined between 473 and 973 K [32,36]. These bands were attributed to different degrees of polymerization of surface monooxo tungstates species. Similarly, one may speculate that the three bands detected by Raman and infrared spectroscopy in the present study are ascribed to different degrees of condensation of surface W species. For W surface densities higher than 1.1 W/nm^2, curve-fitting of the band characteristic of $\nu(W{=}O)$ vibration (Figs. 2b and 5) indicates the presence and the development of the band at 1019–1017 cm^{-1} attributed to most polymerized WO_x species. It must, however, be noted that the Raman band $\nu(W{-}O{-}W)$ characteristic of polymeric W (at ca. 880 cm^{-1}) was not detected. The eventual presence of this band was not noted by in previous Raman in situ studies [20,45] of WO_x/TiO_2 containing between 0.5 and 5.0 W at./nm^2. This may be ascribed to the low Raman scattering cross-section for the $\nu(W{-}O{-}W)$ [34,47]. The detection of this band by infrared is complicated by the strong absorption due to the TiO_2 support for
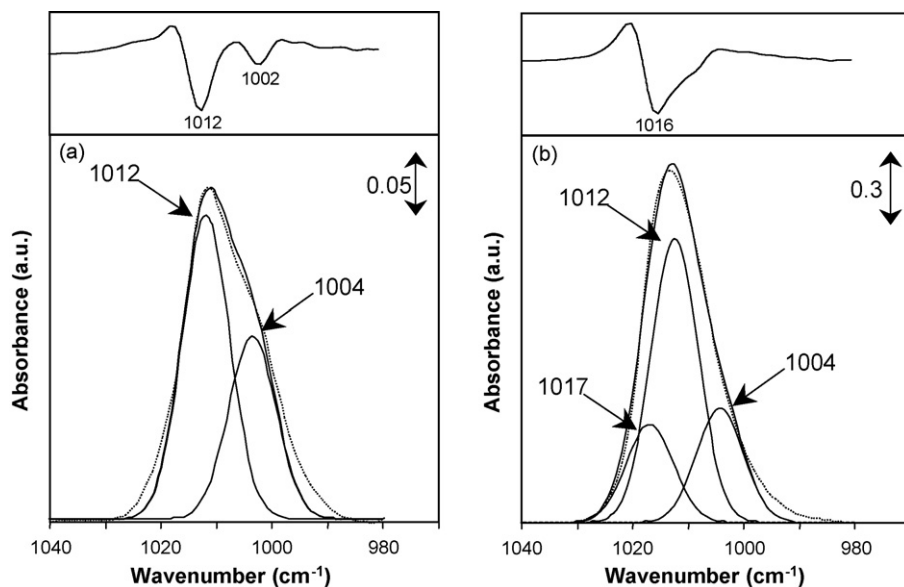
Fig. 4. (Bottom) Curve-fitting of the infrared spectra in the $\nu(W{=}O)$ region for (a) W0.6 T and (b) W3.4 T catalysts. (Top) The 2nd derivatives of these spectra. Dashed line: experimental spectra; full line: curve-fitted spectra.
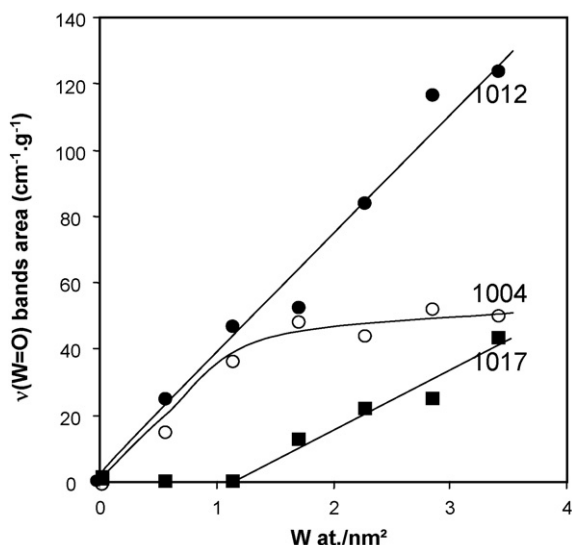
Fig. 5. Evolution of the area of the ν(W=O) bands measured at 1017 (■), 1012 (●) and 1004 (○) cm^{-1} with W surface density of WO_x/TiO_2 solids.

wavenumbers lower than 900 cm^{-1}. The formation of polymeric W species in WO_x/TiO_2 catalysts obtained by pore volume impregnation is confirmed by EXAFS data [46] for W surface densities $\geq$1.6 W at./nm^2.

4.3. Correlation between acidity and catalytic performance

For the sake of clarity, some results of a previous work [35] concerning acidity and catalytic activity are reported in the following section.

4.3.1. Acidity of the surface species

The evolution of the acidity on W deposition was monitored by infrared study of the adsorption of lutidine followed by desorption at various temperatures [35]. The results indicated Brønsted acid sites formation and development on W addition. Such phenomenon has been evidenced by pyridine and ammonia adsorption measurements [10–12,21,34]. Lutidine desorption results at 573 K indicate that a minimum of W surface density (ca. 1.1 at./nm^2) is required for the appearance and development of Brønsted acid sites that are sufficiently strong to retain the probe molecule at this temperature. Similar behaviour has been observed for the WO_x/ZrO_2 system [40].

4.3.2. Catalytic activity

As noted above for Brønsted acidity, catalytic activity measurements show that the development of propene formation activity is only observed above a threshold of W surface density (1.1 at./nm^2). Similar behavior has been reported for tungstated titania prepared from the Ti oxyhydroxide form [36] and for the WO_x/ZrO_2 system [40]. It has also been observed for the reaction of selective catalytic reduction of NO by NH_3 [13] and cumene dealkylation [29] on tungstated titania prepared by impregnation of Ti hydroxide.

4.3.3. Correlation between acidity and catalytic activity

As previously reported [35], a good correlation has been observed between the abundance of "strong" Brønsted acid sites and catalytic activity for isopropanol decomposition. Catalysts containing low W surface densities (<1.7 at./nm^2) were essentially not active and exhibited little or no "strong" Brønsted acid sites (defined as those capable of retaining protonated lutidine species at 573 K). For higher W surface densities, a parallel evolution of the abundance of these acid sites and propene formation activity is observed. A linear relationship (with intercept at the origin) is then found between the concentration of Brønsted acid sites and propene formation activity. Similar results have been observed for the WO_x/ZrO_2 system [40]. They were taken as an indication that the activity of the catalysts for isopropanol dehydration is associated with the development of "strong" Brønsted acid sites.

4.4. Correlation between the nature of the WO_x surface species, the abundance of Brønsted acid sites and the catalytic activity

Fig. 6a shows a good correlation between the number of "strong" Brønsted acid sites determined from lutidine adsorption followed by desorption at 573 K and the area of the infrared band at 1017 cm^{-1} attributed to ν(W=O) vibration associated with the most polymerized WO_x species. The results indicate that, for low W surface densities ($\leq$1.1 at./nm^2), "strong" Brønsted acid sites and highly polymerized W species were not detected. For higher W surface densities, similar evolution of the abundance of these acid sites and that of most condensed W species is observed. This is clearly illustrated in Fig. 6b which shows a linear relationship between these two parameters. Also reported in Fig. 6b is the ensuing linear relationship observed between propene formation rate and the abundance of these W species. Similar correlations were reported for tungstated titania prepared from different precursors and calcined at higher temperatures [36]. Thus, as proposed for the WO_x/ZrO_2 system [40], the formation of "strong" Brønsted acid
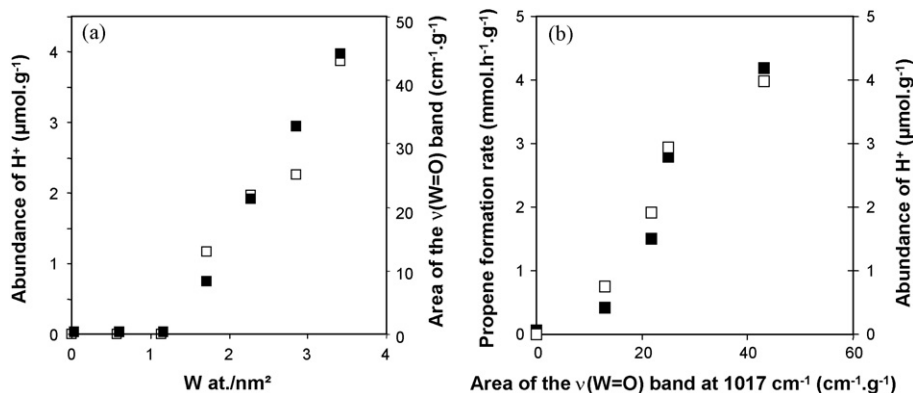

Fig. 6. Correlation between the nature of the WO_x surface species, the abundance of Brønsted acid sites and the catalytic activity: (a) correlation between the number of Brønsted acid sites determined by lutidine desorption at 573 K (■), and the area of the ν(W=O) infrared band located at 1017 cm^{-1} (□); (b) propene formation rate (■) and abundance of Brønsted acid sites determined by lutidine desorption at 573 K (□) vs. the area of the infrared band at 1017 cm^{-1}.
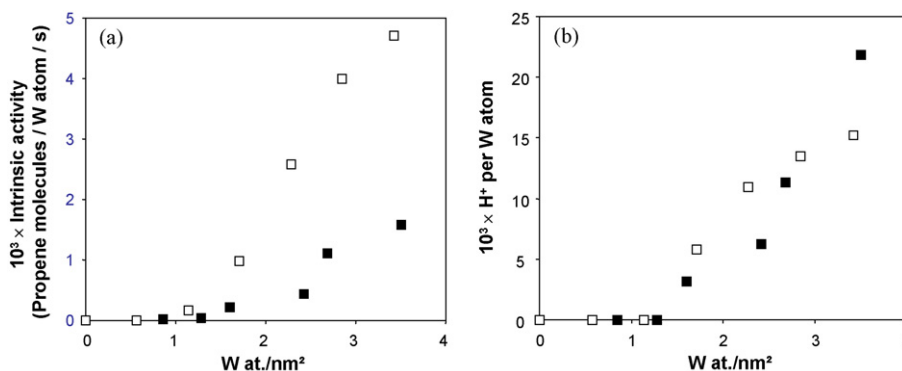
Fig. 7. (a) Activity for propene dehydration at 403 K per W atom vs. W surface density for WO_x/ZrO_2 (■) and WO_x/TiO_2 (□); (b) number of Brønsted acid sites, after desorption of lutidine at 573 K, per W atom for WO_x/ZrO_2 (■) and WO_x/TiO_2 (□).

Table 2
Intrinsic activity for WO_x/TiO_2.

W atom/nm^2	$10^3 \times$ (propene molecules/W atom/s)	Propene molecules/H$^+$/s
1.1	0.18	–
1.7	0.85	0.15
2.3	2.36	0.22
2.8	3.47	0.26
3.4	4.45	0.29

sites appears to be associated with the presence of the most poly-merized WO_x species and the observed activity for isopropanol dehydration.

4.5. WO_x/TiO_2: influence of the crystalline form of the support (anatase vs. rutile)

The WO_x/TiO_2 system used in the present study was obtained by deposition of the W phase over a titania support, consisting of a mixture of anatase and rutile (ca. 60/40). The intrinsic activity for propene formation (per W at.) and the activity per Brønsted acid sites determined by lutidine desorption at 573 K are compared, respectively, in Tables 2 and 3 to those reported in a previous study using pure anatase as a support. The results show, for a given W surface density, higher intrinsic activity for the anatase-supported system. The observed differences in the intrinsic activities may be tentatively attributed to a greater abundance of Brønsted acid sites per W at for anatase-supported system. Indeed both systems exhibit similar activity when normalized to the number of Brønsted acid sites (Tables 2 and 3). However, differences in the pretreatment conditions in those studies, prior to the determination of the abundance of Brønsted acid sites by lutidine desorption, preclude any direct comparison.

4.6. WO_x/TiO_2 and WO_x/ZrO_2: comparison of the two systems

Fig. 7a shows the evolution of the catalytic activity per W atom, designated as "intrinsic" activity, measured at 403 K as a function

Table 3
Intrinsic activity for WO_x/TiO_2 prepared from anatase support. Data derived from Ref. [36].

W atom/nm^2	$10^3 \times$ (propene molecules/W atom/s)	Propene molecules/H$^+$/s
1.3	0.32	–
1.5	1.09	0.12
2.4	4.71	0.21
3.6	7.33	0.27

of W surface density for the WO_x/ZrO_2 [40] and WO_x/TiO_2 systems. Note the parallel evolution of the intrinsic activity of the two systems with W surface density. However, one can readily note that for W surface densities ≥ 1.6 at./nm^2, the intrinsic activity of WO_x/TiO_2 catalysts is ca. threefold higher than that of the corresponding WO_x/ZrO_2 solids. This difference can, in principle, be attributed to lower dispersion (larger cluster size), for a given W surface density, of WO_x/ZrO_2 catalysts. However, Raman results do not suggest any significant differences in the nature of W species. An alternative interpretation would be to attribute the low intrinsic activity of the WO_x/ZrO_2 solids to a lower number of Brønsted acid sites/W atom compared to the corresponding WO_x/TiO_2 system. However, Fig. 7b clearly shows, for both systems, a comparable number of Brønsted acid sites per W atom. It should be noted that the pretreatment temperature of WO_x/TiO_2 catalysts was 100 K lower than that for WO_x/ZrO_2 solids [40]. Thus, one must consider the number of Brønsted acid sites measured for WO_x/TiO_2 catalysts as an upper limit.

One possible explanation for the activity difference may be associated with the inherent limitation of lutidine thermodes-orption as a method for the evaluation of the strength of acid sites. In effect, for a given desorption temperature, these measurements yield the number of Brønsted acid sites sufficiently strong to retain lutidine at this temperature. Thus, one cannot exclude that for a given desorption temperature, WO_x/TiO_2 catalysts prepared from crystalline titania exhibit stronger Brønsted acid sites than the corresponding WO_x/ZrO_2 system. A higher intrinsic activity of WO_x/TiO_2 catalysts as compared to the corresponding zirconia-supported system has been reported by Kim et al. for acid-catalyzed methanol dehydration [37]. This was attributed to a greater acidity of titania-supported surface WO_x species induced by a larger electronegativity of Ti compared to Zr and thus lower electron density of the bridging W–O-support bond (e.g. more acidic).

The difference in activity may also be associated with a greater reducibility of titania-supported W species. In the case of tungstated zirconias, Iglesia and coworkers [48–50] attributed the origin of Brønsted acid sites to a partial reduction of species followed by a stabilisation of the proton on those species. The authors have equally established a relationship between the abundance of partially reduced species, Brønsted acid sites and the activity for butan-2-ol dehydration [48]. Consistent with this hypothesis, one can assume that between two systems, that which is more reducible will exhibit under reaction conditions, more Brønsted acid sites and more activity. Considering that titania-supported surface WO_x species [32,34,51,52] are generally more reducible than those of the corresponding WO_x/ZrO_2 system [34,49,51], one might expect a greater activity for the former system.

5. Conclusions

The surface structure of a series of WO$_x$/TiO$_2$ catalysts containing between 0.6 and 3.4 W at./nm^2 obtained by pore volume impregnation was investigated by X-ray diffraction, Raman and infrared spectroscopy. The results were correlated with the development of relatively strong Brønsted acidity and isopropanol dehydration activity. The following conclusions can be made.

The W phase in all the solids was present as a surface W species. Increasing the W surface density leads to an increased degree of condensation of the W phase. The most condensed W species was characterized by a ν(W=O) vibration at 1017 cm^{-1}.

A minimum of W surface density of 1.1 at./nm^2 appears to be required for the formation of the infrared band at 1017 cm^{-1} attributed to the most condensed W species. A similar threshold was observed for the take off of the activity and the appearance of Brønsted acid sites capable of retaining lutidine following desorption at 573 K.

A direct correlation was observed between propene formation rate and the evolution of the area of the band 1017 cm^{-1}, attributed to the most condensed W species. Furthermore, the abundance of this species appears to be directly related to that of Brønsted acid sites capable of retaining lutidine following desorption at 573 K.

Higher intrinsic activity (activity per W atom) was observed for WO$_x$/TiO$_2$ system as compared to previously reported results for the corresponding WO$_x$/ZrO$_2$ solids.

References

[1] H. Topsoe, B.S. Clausen, F.E. Massoth, in: J.R. Anderson, M. Boudart (Eds.), Catalysis Science and Technology, vol. 11, Springer, Berlin, 1996, p. 1.
[2] J. Ramirez, S. Fuentes, G. Díaz, M. Vrinat, M. Breysse, M. Lacroix, Appl. Catal. 52 (1989) 211.
[3] J.C. Mol, J.C. Moulijn, in: J.R. Anderson, M. Boudart (Eds.), Catalysis Science and Technology, vol. 8, Springer, Berlin, 1987, p. 69.
[4] W. Grünert, R. Feldhaus, K. Anders, E.S. Shpiro, K.M. Minachev, J. Catal. 120 (1989) 444.
[5] S. Meijers, L.H. Gielgens, V. Ponec, J. Catal. 156 (1995) 147.
[6] M. Hino, K. Arata, J. Chem. Soc., Chem. Commun. (1988) 1259.
[7] E. Iglesia, D.G. Barton, S.L. Soled, S. Miseo, J.E. Baumgartner, W.E. Gates, G.A. Fuentes, G.D. Meitzner, in: J.W. Hightower, W.N. Delgass, E. Iglesia, A.T. Bell (Eds.), 11th International Congress on Catalysis—40th Anniversary, Stud. Surf. Sci. Catal., vol. 101, Elsevier, 1996, p. 533.
[8] J. Macht, R.T. Carr, E. Iglesia, J. Catal. 264 (2009) 54.
[9] M. Ai, J. Catal. 49 (1977) 305.
[10] P. Patrono, A. La Ginestra, G. Ramis, G. Busca, Appl. Catal. A 107 (1994) 249.
[11] F. Hilbrig, H. Schmelz, H. Knözinger, in: L. Guszci, F. Solymosi, P. Tétényi (Eds.), New Frontiers Catalysis Proc. 10th ICC, vol. 75, Elsevier, Amsterdam, 1993, p. 1351.
[12] L. Lietti, J. Svachula, P. Forzatti, G. Busca, G. Ramis, C. Bregani, Catal. Today 17 (1993) 131.
[13] J. Engweiler, J. Harf, A. Baiker, J. Catal. 159 (1996) 259.
[14] K. Bourikas, C. Fountzoula, C. Kordulis, Appl. Catal. B 52 (2004) 145.
[15] Y.T. Kwon, K.Y. Song, W.I. Lee, G.J. Choi, Y.R. Do, J. Catal. 191 (2000) 192.
[16] C. Martin, G. Solana, V. Rives, G. Marci, L. Palmisano, A. Sclafani, Catal. Lett. 49 (1997) 235.
[17] T. Yamaguchi, Y. Tanaka, K. Tanabe, J. Catal. 65 (1980) 442.
[18] G.C. Bond, S. Flamerz, L. Van Wijk, Catal. Today 1 (1987) 229.
[19] I.E. Wachs, F.D. Hardcastle, in: M.J. Philips, M. Ternan (Eds.), Proc. 9th I.C.C., vol. 3, 1988, p. 1449.
[20] M.A. Vuurman, I.E. Wachs, A.M. Hirt, J. Phys. Chem. 95 (1991) 9928.
[21] G. Ramis, G. Busca, C. Cristiani, L. Lietti, P. Forzatti, F. Bregani, Langmuir 8 (1992) 1744.
[22] M. Hino, K. Arata, Bull. Chem. Soc. Jpn. 67 (1994) 1472.
[23] J. Papp, S. Soled, K. Dwight, A. Wold, Chem. Mater. 6 (1994) 496.
[24] J.N. Fiedor, M. Houalla, A. Proctor, D.M. Hercules, Surf. Interface Anal. 23 (1995) 234.
[25] D.S. Kim, M. Ostromecki, I.E. Wachs, J. Mol. Catal. A 106 (1996) 93.
[26] N. Vaidyanathan, M. Houalla, D.M. Hercules, Catal. Lett. 43 (1997) 209.
[27] A. Scholz, B. Schnyder, A. Wokaun, J. Mol. Catal. A 138 (1999) 249.
[28] B. Xu, L. Dong, Y. Fan, Y. Chen, J. Catal. 193 (2000) 88.
[29] J.R. Sohn, J.H. Bae, Kor. J. Chem. Eng. 17 (2000) 86.
[30] Z. Ma, W. Hua, Y. Tang, Z. Gao, J. Mol. Catal. 159 (2000) 335.
[31] S. Eibl, R.E. Jentoft, B.C. Gates, H. Knözinger, Phys. Chem. Chem. Phys. 2 (2000) 2565.
[32] S. Eibl, B.C. Gates, H. Knözinger, Langmuir 117 (2001) 107.
[33] X.F. Yu, N.Z. Wu, H.–Z. Huang, Y.C. Xie, Y.Q. Tang, J. Mater. Chem. 11 (2001) 3337.
[34] A. Gutiérrez-Alejandre, P. Castillo, J. Ramirez, G. Ramis, G. Busca, Appl. Catal. A 216 (2001) 181.
[35] T. Onfroy, G. Clet, S.B. Bukallah, T. Visser, M. Houalla, Appl. Catal. A 298 (2006) 80.
[36] V. Lebarbier, G. Clet, M. Houalla, J. Phys. Chem. B 110 (2006) 22608.
[37] T. Kim, A. Burrows, C.J. Kiely, I.E. Wachs, J. Catal. 246 (2007) 370.
[38] G.D. Panagiotou, T. Petsi, K. Bourikas, C. Kordulis, A. Lycourghiotis, J. Catal. 262 (2009) 266.
[39] R.B. Quincy, M. Houalla, D.M. Hercules, Fresenius J. Anal. Chem. 346 (1993) 676.
[40] T. Onfroy, G. Clet, M. Houalla, J. Phys. Chem. B 109 (2005) 3345.
[41] T. Onfroy, G. Clet, M. Houalla, Micropor. Mesopor. Mater. 82 (2005) 99.
[42] B. Zhao, X. Xu, J. Gao, Q. Fu, Y. Tang, J. Raman Spectrosc. 27 (1996) 549.
[43] N. Vaidyanathan, M. Houalla, D.M. Hercules, Surf. Interface Anal. 26 (1998) 415.
[44] R.M. Pittman, A.T. Bell, J. Phys. Chem. 97 (1993) 12178.
[45] S.S. Chan, I.E. Wachs, L.L. Murrell, L. Wang, W.K. Hall, J. Phys. Chem. 88 (1984) 5831.
[46] F. Hilbrig, H.E. Göbel, H. Knözinger, H. Schmelz, B. Lengeler, J. Phys. Chem. 95 (1991) 6973.
[47] G. Busca, J. Raman Spectrosc. 33 (2002) 348.
[48] C.D. Baertsch, K.T. Komala, Y.H. Chua, E. Iglesia, J. Catal. 205 (2002) 44.
[49] D.G. Barton, S.L. Soled, G.D. Meitzner, G.A. Fuentes, E. Iglesia, J. Catal. 181 (1999) 57.
[50] D.G. Barton, M. Shtein, R.D. Wilson, S.L. Soled, E. Iglesia, J. Phys. Chem. B 103 (1999) 630.
[51] J.N. Fiedor, A. Proctor, M. Houalla, D.M. Hercules, Surf. Interface Anal. 23 (1995) 204.
[52] D.C. Vermaire, P.C. van Berge, J. Catal. 116 (1989) 309.